Region multi-center method for land use classification of multispectral RS imagery

LIN Jian[1,2], ZHONG Ying-chun[2], PENG Shun-xi[3], LIU Jian-xun[1]

1. *Laboratory of Knowledge Grid, Hunan University of Science & Technology, Hunan Xiangtan* 411201, *China*;
2. *Department of Geographical Information System, Hunan University of Science and Technology, Hunan Xiangtan* 411201, *China*;
3. *School of Info-physics and Geomatics Engineering, Central South University, Hunan Changsha* 410083, *China*

Abstract: A convenient multivariate statistical model is in general not available for the multi-spectral feature of land use (LU) class of remote sensing (RS) image, as one LU class is made up of several ground objects. Analyzing the spectral characteristics of LU of multispectral RS imagery, this paper presents a rule-based region multi-center (RMC) method. In the method, the classification cell is pixel region, the classificatory pattern is a set of the classificatory intra-class centers which is confirmed by clustering the training samples, and the classification rules are the type amounts of intra-class center and the percentage of the pixels belonged to the class from the whole region pixels. RMC method can also be used to recognize the individual LU class from multi-spectral RS image. This method deals with the distribution problem by multi-center and based on rule method. There are much difference of the classificatory center amount and the pixel's percentage among different LU class, so the selection of training area and the determinants of rules are easy. The results of experiment indicate that the LU classification accuracy is increased between 4% and 6% with this method.

Key words: multispectral remote sensing imagery, land use classification, region multi-center (RMC)

CLC number: TP79 **Document code:** A

Citation format: Lin J, Zhong Y C, Peng S X and Liu J X. 2010. Region multi-center method for land use classification of multispectral RS imagery. *Journal of Remote Sensing*. 14(1): 165—179

1 INTRODUCTION

LU categories are classified by the aims of human activity (Yuan *et al.*, 2005; Zhu, 2006), and there are many types of ground material in one land use class. LU classification from RS imagery is based on the spectral features of ground objects, so there is different material spectrum in the same LU class. Using multispectral RS imagery for LU classification, a convenient multivariate statistical model is in general not available for the multispectral characteristics of LU class (Alberti *et al.*, 2004; Gislason *et al.*, 2005).

So there are mainly three solutions: firstly, try best to make the samples satisfy the multivariate statistical distribution, such as with the unsupervised clustering method, to choose the dominant and continuous pixels as training samples, then classify with statistical pattern recognition method (Kuemmerle *et al.*, 2006; Benediktsson *et al.*, 1997). Though this solution reduces the differences of samples, the training samples don't contain all ground objects' information. So the difference between classificatory pattern and the ground object is rather great to result in classification error (Lin *et al.*, 2002, Cabido & Zak, 2002).

Secondly, make use of elevations, textures, boundaries and all other secondary information to reduce the dependence on the spectral information, whereas the secondary information add the dimension of the classification feature vector, and the vector multivariate statistical model is more difficult available. So we commonly adopt multi-classifier confusion method to classify different types of information, to reduce the classification vector dimensions of single classifier and improving the clustering performance of the classification vector, then fuse the results of several classifiers (Lin *et al.*, 2004; Bruzzone *et al.*, 2004; Cingolania *et al.*, 2004). However, the problem of spectral information statistical distribution is not taken account in these methods, the classification accuracy increases is limited, even it may lower to some classes (Smith *et al.*, 2003).

Thirdly, take the un-statistical pattern recognition method to solve multivariate statistical distribution, such as decision tree method. This method makes use of the class subset to form the

Received: 2008-01-07; **Accepted**: 2008-10-30

Foundation: The Natural Science Foundation of China (No. 60673119), the Natural Science Foundation of HUNAN Provincial (No. 07JJ5066), Foundation of Hunan Provincial Development and Reformation Committee (No. 149, 2008), Foundation of Hunan Provincial Education Department (No. 06C313).

First author biography: LIN Jian (1964—), male, vice-professor, graduated from geo-exploration and info-technology specialty of Central South University, mainly engaged in pattern recognition, remote sensing image processing research work. He has published about 20 scientific papers. E-mail: lj2110015@163.com

boundary of branch decision tree (Lucas *et al.*, 2007; Zhao *et al.*, 2005; Conese *et al.*, 1993), but it is difficult to divide subset and to form rules for the method.

Analyzing the multi-spectral feature of LU in RS image, this paper presents a new method, Region Multi-Center (RMC), for LU classification of multi-spectral RS image. In this method, the classification cell is region, classificatory pattern is formed by clustering centers of training samples, and adopt rule-based method to classify.

2 MULTI-SPECTRAL FEATURE ANALYSIS OF RS IMAGERY

2.1 Intra-class distance distribution

Considering that designing classifier is based on the distance distribution between feature vector and the classificatory center vector, and LU class is made up of several types of ground objects, we study the distance distribution between the intra-class center vectors and the LU classificatory center vector.

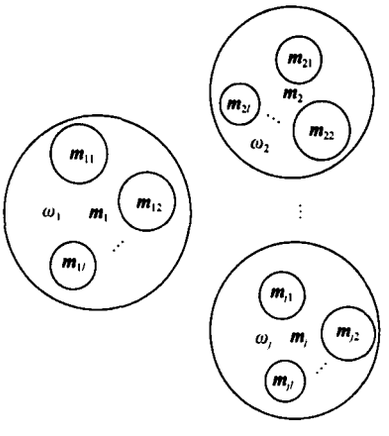

Fig. 1 Sketch of classificatory centers and intra-class centers

Suppose that the training sample set of c classes is $\{\boldsymbol{x}_1, \boldsymbol{x}_2, \cdots, \boldsymbol{x}_N\}$, where c is the number of object classes, and $\boldsymbol{x}_i$ represents the feature vector of training sample i. The sample set of class ω_j is $\{\boldsymbol{x}_i^{(j)}; j=1,2,\cdots,c; i=1,2,\cdots,n_j\}$, and the superscript j denotes class, lower-script i denotes serial number of the samples, n_j is the number of class ω_j samples, and $\sum_{j=1}^{c} n_j = N$, the center vector of class ω_j adopts the mean vector $\boldsymbol{m}_j$, and $\boldsymbol{m}_j = \frac{1}{n_j}\sum_{i=1}^{j} \boldsymbol{x}_i^{(j)}, j=1,2,\cdots,c$. Cluster the training samples of class ω_j by the distance threshold method to form k intra-class centers (as Fig. 1), which are represented by $\{\omega_{j1}, \omega_{j2}, \cdots, \omega_{jl}\}, l=1,2,\cdots,k$. The sample set of intra-class center ω_{jl} is $\{\boldsymbol{x}_i^{(jl)}; j=1,2,\cdots,c; l=1,2,\cdots,k; i=1,2,\cdots,n_l\}$, where ω_{jl} represents the l th intra-class center of class ω_j, n_l is the number of samples of intra-class center ω_{jl}, and $\sum_{l=1}^{k} n_l = n_j$. The mean vector of intra-class centers is $\{\boldsymbol{m}_{j1}, \boldsymbol{m}_{j2}, \cdots, \boldsymbol{m}_{jl}\}, l=1,2,\cdots,k$, and $\boldsymbol{m}_{jl} = \frac{1}{n_l}\sum_{i=1}^{n_l} \boldsymbol{x}_i^{(jl)}$, $j=1,2,\cdots,c; l=1,2,\cdots,k$. The distance between class ω_j center and its intra-class ω_{jl} centers is $d_{jl} = \|\boldsymbol{m}_{jl} - \boldsymbol{m}_j\|$. The intra-class distance distribution can be represented with the graph that setting the percentage of n_l/n_j as the y-axis and setting the d_{jl} as the x-axis.

2.2 Multi-spectral feature of LU class

Select samples from urban land, woodland, plantation land and water four classes of LU in Landsat TM (Bands 4, 3, and 2) image of Changsha, to analyze the intra-class distance distribution of multi-spectrum. The rule of selecting samples is that samples should cover as many pixels of ground objects as possible, and the distribution range of samples should be wide. According to the rule, choose 8192 pixels in each class respectively. Fig. 2 shows the rough region of samples.

Fig. 2 Rough region of samples in the RS image

Fig. 3 shows the graph of intra-class distance distributing of LU class, and the distance threshold of max-minimum clustering is 30. From Fig. 3, we can know: (1) The spectral value of pixels in every class has many intra-class centers. (2) Each class exists several relatively concentrated distance intervals, such as 30—40 and 60—70 of water. It represents that one class of LU is composed of several mainly ground material. (3) Spatial distance distribution of water is the most concentrated, and the distribution of urban land is more concentrated than that of woodland and plantation land, but the continuity of urban land is less than woodland and plantation land.

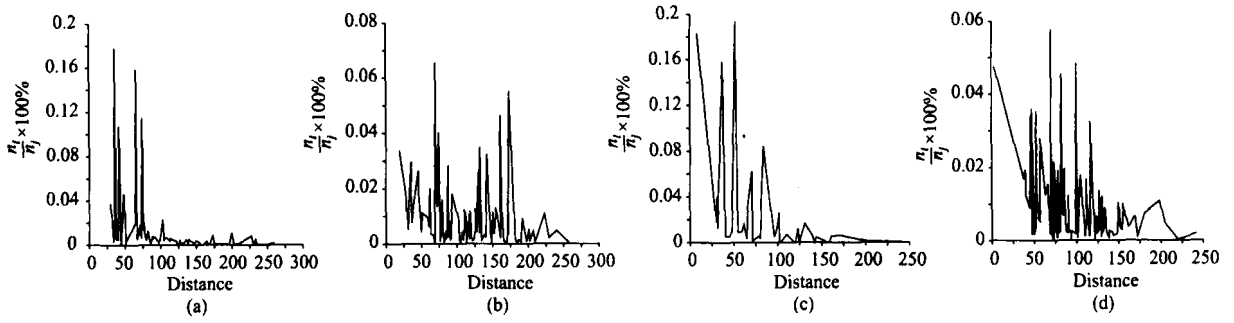

Fig. 3 Graph of spatial distance distributing of LU class
(a) Water; (b) Woodland; (c) Urban land; (d) Plantation land

3 RMC METHOD

3.1 Basic thought of the method

LU classification rules are the type of ground objects and their ratio of area by whole area of object cell, such as the city' criterion of level-1 class is that the area of building and traffic should be more than two thirds, and any other LU area should not be more than one third of the total area. According to the thought of classification, the basic thought of the method of RS image classification for LU is as follow: (1) take pixel region as classification cell, (2) take thresholds that relate to the ground objects as classification rules. As Fig. 4 shows a 5×5 region cell in urban land area, if $\omega_{31},\omega_{33},\omega_{34},\omega_{39}$ denote building, road, wood and water, respectively, the region cell has four ground objects types of LU class, and the total pixels in urban land is 18, and the ratio to the total region pixels is 72%.

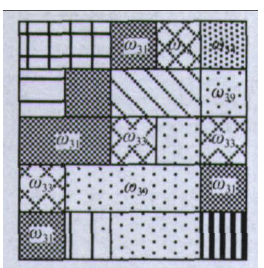

Fig. 4 Sketch of classificatory object types in the region cell

In view of that the intra-class distance distribution reflects on the spectral feature of LU class (Fig. 3), a method of RS image classification of LU is presented. In the method, the classification cell is pixel region, the classificatory pattern is a set of the classificatory intra-class centers, and the classification rules are the type amounts of intra-class center and the percentage of the pixels belonged to the class from the whole region pixels. This classification method is called RMC method.

3.2 Confirming classificatory pattern

With a set of intra-class centers representing a classificatory pattern of LU, the number of centers is the key to determine the classificatory pattern, and the principle of selecting classificatory pattern is that: the distance of intra-class should be the minimum, and the inter-class distance should be the maximum. So we choose the number of centers by calculating the intra-class and inter-class distance of classificatory pattern.

As shown in Fig. 1, with single center representing classificatory pattern, the function of intra-class distance is following:

$$d_{\omega} = \sum_{j=1}^{c}\sum_{i=1}^{n_j}\left\| \boldsymbol{x}_i^{(j)} - \boldsymbol{m}_j \right\|^2$$

where $\boldsymbol{m}_j$ is the mean-vector of class ω_j classificatory pattern. The function of inter-class distance is defined as follows:

$$d_B = \frac{1}{c}\sum_{j=1}^{c}(\boldsymbol{m}_j - \boldsymbol{m})'(\boldsymbol{m}_j - \boldsymbol{m})$$

where $\boldsymbol{m}$ is the mean-vector of all the patterns and $\boldsymbol{m} = \frac{1}{N}\sum_{i=1}^{N}\boldsymbol{x}_i$.

With a set of intra-class centers representing classificatory pattern, the function of multi-center intra-class distance is $d_{\omega\omega} = \sum_{j=1}^{c}\sum_{i=1}^{n_j}\left\| \boldsymbol{x}_i^{(jl)} - \boldsymbol{m}_{jl} \right\|^2$, and the function of multi-center inter-class distance is $d_{B\omega} = \frac{1}{c\times k}\sum_{j=1}^{c}\sum_{l=1}^{k}(\boldsymbol{m}_{jl} - \boldsymbol{m})'(\boldsymbol{m}_{jl} - \boldsymbol{m})$, where $\boldsymbol{m}_{jl}$ is the mean vector of intra-class center ω_{jl}.

With C-mean clustering method and the samples of experiment in Section 1.2, the multi-center intra-class and inter-class distance of samples are shown in Table 1.

Select the center number based on the principle of the minimum intra-class distance and the maximum inter-class distance. The number of centers can range from 10 to 120 in accordance with Table1.

3.3 RMC feature of LU

We make use of two types of RMC features, one is that the region cell has the type's amount of classificatory intra-class center, the other is that the ratio of classificatory pixels to the total pixels of region cell. The method of these feature acquired is as follows:

(1) Cluster classificatory training samples to form the multi-center by C-mean method. Then delete the center of which pixel number is less a threshold, to exclude imagery

Table 1 Intra- and inter-class distances of different numbers of intra-class center

Center amount	1	2	5	10	25	30	50	100	120	200
Intra-class distance	76.91	78.97	61.85	40.16	28.71	25.45	18.97	13.67	12.99	9.60
Inter-class distance	103.42	31.38	71.18	109.59	108.53	102.61	128.14	112.49	147.51	97.34

noise and the influence of ground objects including the least pixels. At last, take the set of adjusted centers for classificatory pattern, and calculate the minimum distance $d_{\min}$ between the pixel and the center.

(2) Select region size arbitrarily in classes, cluster the pixels of region by distance threshold value $d_{\min}$, i.e. if $\|x - m_{jl}\| \leqslant d_{\min}$, so $x \in \omega_{jl}$, and calculate the amount of region cell containing intra-class center ω_{jl} of class ω_j.

(3) Calculate the ratio of classificatory pixels to the total pixels of region cell.

3.3.1 RMC feature of different training samples

According to the principles in paragraph 2.2, select A, B, and C three group samples, and these sample's amount are 8192, 4096, and 1024 pixels, respectively. The original class amount of C-mean clustering is 50. Delete centers of which pixels are less than 0.1% of the total training samples. Then, select arbitrarily a 11×11 region cell from each class. Multi-center features of the region cell are shown in Table 2 and Table 3.

To different training samples, Table 2 and Table 3 show obviously that: the number of intra-class centers and the pixel percentage to the category that region cell comes from are far more than to other categories.

3.3.2 RMC feature in different size of region cell

In sample group C, select 16×16 and 7×7 region cell respectively. Multi-center features of the region cells are shown in Table 4 and Table 5.

To different region cell size, Table 3 to Table 5 shows obviously that: the number of intra-class centers and the pixel percentage to the category that region cell comes from are far more than to other categories.

3.4 Method steps

Fig. 5 shows the steps of RMC method for LU classification of multispectral RS imagery.

Table 2 RMC feature of the region cell of training samples group A

	Water samples	Woodland samples	Urban land samples	Plantation samples
Water	10, 100%	0, 0	2, 21.9%	0, 0
Woodland	0, 0	6, 100%	3, 23.5%	1, 7.4%
Urban land	0, 0	1, 3.3%	19, 100%	0, 0
Plantation land	0, 0	0, 0	3, 4.1%	11, 100%

Note: The front denote the classificatory intra-class center amount, the back denote the percent of pixels.

Table 3 RMC feature of the region cell of training samples group C

	Water samples	Woodland samples	Urban land samples	Plantation samples
Water	14, 100%	0, 0	4, 19.8%	0, 0
Woodland	0, 0	8, 100%	2, 29.7%	1, 0.8%
Urban land	0, 0	0, 0	25, 100%	0, 0
Plantation land	1, 0.8%	0, 0	2, 3.2%	11, 95.0%

Table 4 RMC feature of the region cell size 16×16

	Water samples	Woodland samples	Urban land samples	Plantation samples
Water	23, 99.6%	0, 0	0, 0	2, 15.6%
Woodland	0, 0	10, 97.6%	0, 0	0, 0
Urban land	4, 51.1%	2, 41.5%	27, 98.4%	3, 4.7%
Plantation land	0, 0	4, 3.9%	0, 0	25, 98.8%

Table 5 RMC feature of the region cell size 7×7

	Water samples	Woodland samples	Urban land samples	Plantation samples
Water	10, 100%	0, 0	0, 0	2, 6.1%
Woodland	0, 0	4, 93.0%	0, 0	0, 0
Urban land	2, 38.7%	2, 40.0%	19, 100%	0, 0
Plantation land	0, 0	0, 0	0, 0	12, 100%

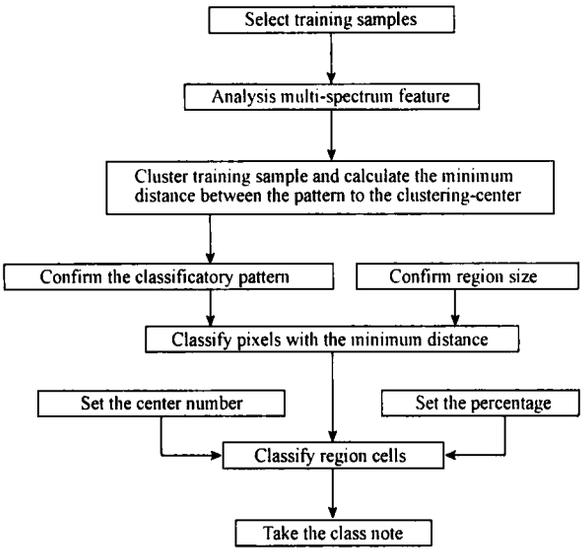

Fig. 5 Flowchart of RMC method

4 EXPERIMENT

The experiment data is shown in Fig. 2. Select urban land, woodland, plantation land, water and bare land five level-1 classes of LU to classify. In the classified images, the five classes are marked with green, red, yellow, blue and white, respectively, and the undivided regions are marked with black.

All kinds of classification method adopt identical method of training sample choice and accuracy evaluation. The principle of selecting training samples is that: samples should cover as many pixels of all ground objects in LU as possible, and the distribution range of samples should be wide. The method of accuracy evaluation is as follows: choose 100 points in the classified image at random and calculate the classification error according to the result maps of visual interpretation method.

4.1 Classification of general methods

Fig. 6 shows the results of general methods of LU classification. Fig. 6(a), 6(b), 6(c) and 6(d) express the maximum-likelihood method (Benediktsson *et al.*, 1997), the FasART neural network method (Lin *et al.*, 2002), the decision tree method (Zhao, *et al.*, 2005) and the method of combining region features and spectral information by multi-classifiers, respectively. The classification accuracy is shown in Table 6.

From Table 6, to woodland and plantation land class, the accuracy of classification methods of neural network and decision tree are better than the method of maximum likelihood, that is because spectral features of these classes are relatively dispersal. The accuracy of fusion classification method based on the region and spectral information increases but not high.

4.2 RMC method with different rules

The size of region cells is 5×5, and the classification center is formed by training samples in group A. The center amount of the urban land, water, plantation land, woodland and bare land are 50, 20, 50, 50 and 10, respectively, The result maps of experiment with different center amount and percentage thresholds are shown in Fig. 7, and the classification accuracy is shown in Table 7.

As shown in Fig. 7(d), when the threshold of center amount is 2, the unclassified region increases obviously, but the classification accuracy does not change largely. There are two reasons, one is that the pixels in the small region are relatively concentrated, on the other hand is that the judge distance is small, when the number of cluster centers is large. From Table 7, we know that the accuracy change due to the change of threshold is less than 1%. Therefore, it is easy to select the threshold of classification rules. Compared to Fig. 6, the spots

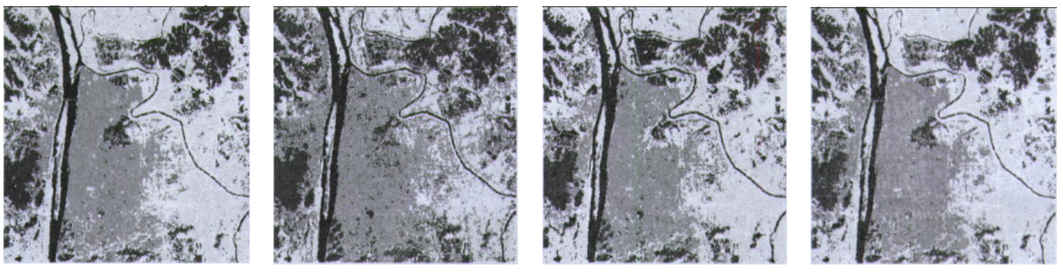

(a) (b) (c) (d)

Fig. 6 Result map of general classification methods for LU

(a) Maximum-likelihood; (b) Neural network; (c) Decision tree; (d) Combining region and spectrum information by multi-classifiers

Table 6 Classification accuracy of general methods/%

Classification method	Water	Woodland	Urban land	Plantation land	Bare land	Average accuracy
Maximum-likelihood	85.6	84.1	76.3	82.9	86.5	83.08
Neural network	87.7	86.8	72.4	85.6	85.3	83.56
Decision tree	90.2	85.7	74.6	84.2	85.1	83.96
Fusion classification	87.0	85.2	81.7	84.1	85.9	84.78

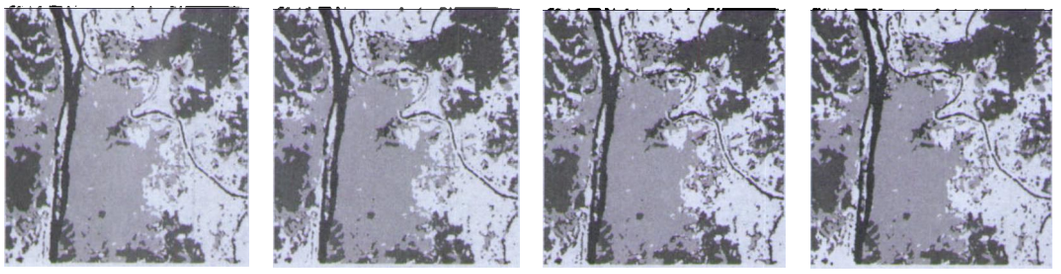

(a) (b) (c) (d)

Fig. 7 Classification result map of RMC method with different threshold of center amount and percent
(a) Center amount is 1, percent is 50%; (b) Center amount is 1, percent is 55%; (c) Center amount is 1, percent is 60%; (d) Center amount is 1, percent is 45%

Table 7 Classification accuracy of different threshold of center amount and percent/%

Fig. 7	Water	Woodland	Urban land	Plantation land	Bare land	Average accuracy
(a)	87.5	88.3	86.8	88.7	85.9	87.44
(b)	87.1	88.9	87.7	89.1	85.7	87.70
(c)	87.5	87.8	86.8	88.8	86.0	87.38
(d)	87.3	87.5	86.6	88.0	85.2	86.92

decrease obviously in Fig. 7, meanwhile, the classification accuracy increases approximately 4% in Table 7 compared to Table 6.

4.3 Classification with different training samples and classificatory patterns

Fig. 8 reflects the classification results of different training samples and different center amount of the same training samples. The region cell is with a size of 5×5, the threshold of center amount and percentage are 1 and 55%, respectively. Table 8 shows the classification accuracy. Fig. 8(a)—Fig. 8(c) is the classification result maps of group B with different center amount of sample pattern. It is difficult to detect the classification difference from the maps. In Table 8 the accuracy error difference is less than 0.5%, so it fully indicates that the changes of center amount have a little effect on classification accuracy. There are three groups of training samples in Fig. 7 and Fig. 8, and the mean accuracy difference does not surpass 1% in accordance with Table 7 and Table 8. All these prove that the request of choosing training samples is not strict for RMC method.

4.4 Single class recognition of RMC method

Fig. 9 shows the results of single class recognition of RMC method. In classification process, we only choose the training samples from single class. According to the result maps, there is nearly no spots in the class and it is similar with the results of the land level-1 classification by visual RS image. The parame-

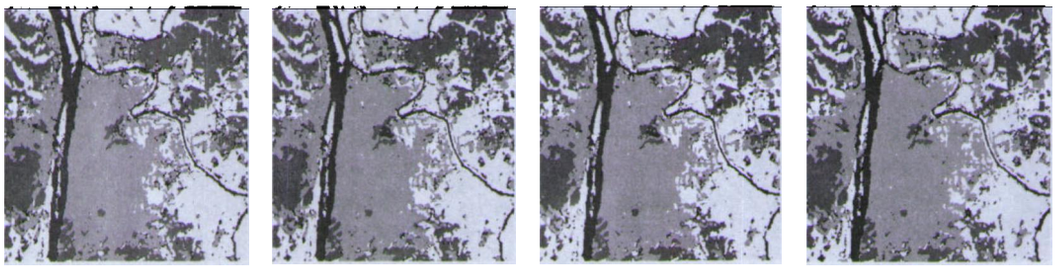

(a) (b) (c) (d)

Fig. 8 Classification result map of RMC method with different training samples and classificatory pattern
(a) Group B, pattern is 50,20,50,50 and 10; (b) Group B, pattern is 50,30,70,70 and 20; (c) Group B, pattern is 60,30,60,60 and 20; (d) Group C, pattern is 50,20,50,50 and 10

Table 8 Classification accuracy of different training samples and classificatory pattern/%

Fig. 8	Water	Woodland	Urban land	Plantation land	Bare land	Average accuracy
(a)	88.5	87.8	86.8	89.3	86.2	87.72
(b)	88.2	87.6	87.0	88.9	85.3	87.40
(c)	87.9	88.3	86.4	89.2	86.0	87.56
(d)	86.4	88.5	88.7	89.0	84.1	87.34

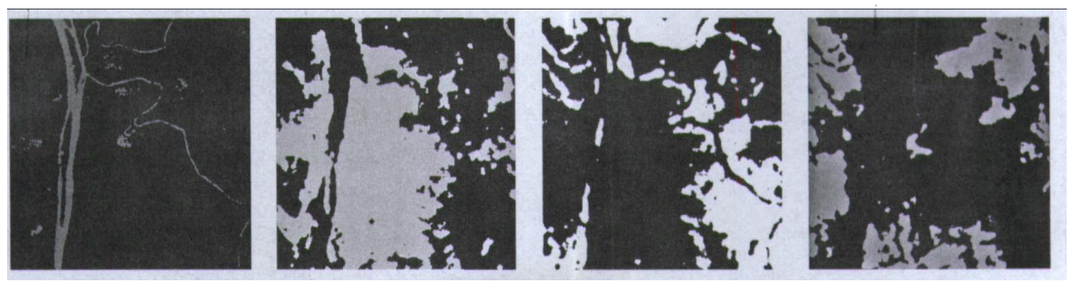

Fig. 9 Result map of recognizing the individual LU class with RMC method
(a) Water; (b) Urban land; (c) Plantation land; (d) Woodland

Table 9 Accuracy and different parameters of recognizing the individual LU class with RMC method

	Region cell size	Pattern center	Center Amount	Percentage	Accuracy/%
Water	3×3	20	1	55	89.6
Urban land	11×11	50	3	60	90.1
Woodland	9×9	50	4	60	89.7
Plantation land	9×9	50	3	60	91.2

ters of RMC method and classification accuracy are listed in Table 9. Comparing with Table 7 and Table 8, we know that the accuracy of every class increases, and the mean accuracy increases about 3%. This is because that we can select different region cell size according to the scale feature of classes, and if the size of classification region enlarges, it can help control the threshold of center amount to increase the classification accuracy.

5 CONCLUSION

This paper presents a RMC method for LU classification of multispectral RS imagery. The classification cell is region, and the classificatory pattern is represented by intra-class center set of the training samples. The method fully considers the characteristics that a kind of LU class is covered with several ground objects, and the classificatory pattern does not meet multivariate statistical distribution. To RMC method, the multispectral feature is more dispersal, the classification accuracy is improved greatly. There are two classification rules of RMC method, one is the type amount of classificatory intra-class centers which the pixel of the region cell belonged to, the other is the percentage of the pixels belonged to the class from the whole region cell pixels. The rules express sufficiently the basic idea of LU classification system and classification based on the area ratio of ground objects to whole region. Meanwhile, it fuses the region information and the spectral information. Owing to the large difference of RMC feature, it is simple to establish the classification rules and to select training samples. RMC method which multi-centers confirmed by clustering solve preferably the problems of the division of subset and the confirmation of boundary of decision tree method. Furthermore, the method can be applied to single class recognition and can adopt different classification rules for different classes. RMC method can increase the LU classification accuracy of multispectral RS imagery between 4% and 6%.

REFERENCES

Alberti M, Weeks R and Coe S. 2004. Urban land cover change analysis in Central Puget Sound. *Photogrammetric Engineering and Remote Sensing*, **70**(9): 1043—1052

Benediktsson J A, Sveinsson J R and Swain P H. 1997. Hybrid consensus theoretic classification. *IEEE Trans. Geosci. Remote Sens*, **35**(4): 833—843

Bruzzone L, Cossu R and Vernazza G. 2004. Detection of land-cover transitions by combining multidate classifiers. *Pattern Recognition Letters*, **25**(13): 1491—1500

Chen Q X, Luo J C, Zhou C H, Zheng J, Lu X J and Shen Z F. 2004. Classification of remotely sensed imagery using multi-features based approach. *Journal of Remote Sensing*, **8**(3): 239—245

Cingolania A M, Renisona D, Zak M R and Cabido M R. 2004. Mapping vegetation in a heterogeneous mountain rangeland using landsat data: an alternative method to define and classify land-cover units. *Remote Sensing of Environment*, **92** (1): 84—97

Conese C, Gilabert M A, Maselli F and Bottai L. 1993. Topographic normalization of TM scenes through the use of an atmospheric correction method and digital terrain models. *Photogrammetric Engineering and Remote Sensing*, **59**(12): 1745—1753

Gislason P O, Benediktsson J A and Sveinsson J R. 2006. Random Forests for land cover classification. *Pattern Recognition Letters*, **27**(2): 294—300

Kuemmerle T, Radeloff V C, Perzanowski K and Hostert R. 2006. Cross-border comparison of land cover and landscape pattern in Eastern Europe using a hybrid classification technique. *Remote Sensing of Environment*, **103**(1): 449—464

Lin J, Bao G S, Jing R Z and Huang J X. 2002. A study of fasART neuro-fuzzy networks for supervised classification of remotely

sensed images. *Journal of Image and Graphics*, **7**(12): 186—190

Lin J, Bao G S, Wang R S and Wang X. 2004. Fusion spectrum and texture information of RS image based on decomposing fuzzy density. *Acta Electronica Sinica*, **32**(12): 2028—2030

Lucas R, Rowlands A, Brown A, Keyworth S and Bunting P. 2007. Rule-based classification of multi-temporal satellite imagery for habitat and agricultural land cover mapping. *ISPRS Journal of Photogrammetry & Remote Sensing*, **62**(3): 165—185

Luo J C, Wang Q M, Ma J H, Zhou C H and Liang Y. 2002. The EM-based maximum likelihood classifier for remotely sensed data. *Acta Geodaetica Et Cartographic Sinica*, **31**(3): 234—239

Min X, Pakorn W V and Manoj K A. 2005. Decision tree regression for soft classification of remote sensing data. *Remote Sensing of Environment*, **97**(3): 322—336

Pal M and Mather P M. 2003. An assessment of the effectiveness of decision tree methods for land cover classification. *Remote Sensing of Environment*, **86**(3): 554—565

Smith J H, Stehman S V, Wickham J D and Yang L M. 2003. Effects of landscape characteristics on land-cover class accuracy. *Remote Sensing of Environment*, **84**(2): 342—349

Yuan F, Sawaya K E, Brian C and Bauer M E. 2005. Land cover classification and change analysis of the Twin Cities (Minnesota) Metropolitan Area by multitemporal Landsat remote sensing. *Remote Sensing of Environment*, **98**(2): 317—328

Zak M R and Cabido M. 2002 Spatial patterns of the Chaco vegetation of central Argentina: Integration of remote sensing and phytosociology. *Applied Vegetation Science*, **5**(2): 213—226

Zhao P, Fu Y F, Zheng L G and Feng X Z. 2005. Cart-based land use/cover classification of remote sensing image. *Journal of Remote Sensing*, **9**(6): 708—716

Zhu H J. 2006. Research on classification and representation of residential change for the automatic retrieval incremental information. *Journal of Hunan University of Science & Technology*, **21**(3): 65—68

多光谱遥感图像土地利用分类区域多中心方法

林　剑[1,2], 钟迎春[2], 彭顺喜[3], 刘建勋[1]

1. 湖南科技大学 知识网格实验室, 湖南 湘潭　411201;
2. 湖南科技大学 地信系, 湖南 湘潭　411201;
3. 中南大学 信息物理工程学院, 湖南 长沙　410083

摘　要: 针对遥感图像土地利用一种类别由多种地物组成, 存在难以求取类别光谱特征多元分布模型的问题, 分析了多光谱遥感图像土地利用的光谱特征和区域多中心特征, 提出了一种光谱信息和区域信息基于规则的区域多中心分类方法, 以类别的类内中心集合表征类别模式, 以区域为分类单元, 以区域单元含类别类内中心数和区域单元中属于某种类别的像元占单元总像元的百分比为分类准则; 采用类内中心表征类别模式和基于规则的分类方法, 较好地解决了土地利用类别由多种地物组成、类别模式不满足多元正态分布的问题, 由于类别区域单元多中心特性差异大, 分类规则的建立及训练样本的选择易于实现。实验表明: 该方法能提高分类精度 4%—6%。

关键词: 多光谱遥感图像, 土地利用分类, 区域多中心

中图分类号: TP79　　**文献标识码:** A

引用格式: 林　剑, 钟迎春, 彭顺喜, 刘建勋. 2010. 多光谱遥感图像土地利用分类区域多中心方法. 遥感学报, 14(1): 165—179
Lin J, Zhong Y C, Peng S X and Liu J X. 2010. Region multi-center method for land use classification of multispectral RS imagery. *Journal of Remote Sensing*. 14(1): 165—179

1　引　言

土地利用是指人类施加于地表的活动, 是基于人类活动的影响程度及活动目的进行划分的(Yuan 等. 2005, 朱华吉, 2006), 土地利用类别属于信息类别。多光谱遥感图像地物分类是以地物的光谱特征为依据的, 地物类别属于光谱类别。利用多光谱遥感图像直接进行土地利用分类, 存在一种土地利用类型由多种地物组成, 在多光谱遥感图像上同一类别具有不同的光谱值, 分类时难以求取类别光谱特征的多元统计分布模型(Alberti 等, 2004, Gislason 等, 2005)。

为此, 主要采用 3 种途径解决, 一是尽可能使训练样本满足多元统计分布, 如先用非监督分类进行聚类, 选取类别中占优势连续的像元块作为训练样本, 然后用统计模式识别的方法分类(Kuemmerle 等, 2006, Benediktsson 等, 1997), 该类方法通过训练样本的选取, 压制样本之间的差异求取光谱特征分布模型, 但训练样本未能包含土地利用类别的全部地物信息, 所形成的类别模式与类别实际组成有较大的偏差而造成分类误差(林剑等, 2002, Zak & Cabido, 2002); 二是利用辅助信息减少对光谱信息的依赖, 如地形高程、土壤含水、纹理及其他空间结构信息等, 但存在辅助信息与遥感图像的一致性、辅助信息与类别的规律性的问题(陈秋晓等, 2004, 骆剑永等, 2002), 同时, 辅助信息的加入增大了分类矢量的维数, 使类别特征更难以满足多元统计分布, 通常采用分类器融合的方法分别对不同类型的信息分类, 以减少单一分类器中的分类矢量维数及改善类别矢量的聚类性能, 然后融合多个分类器分类的结果(林剑等, 2004, Bruzzone 等, 2004, Cingolania 等, 2004), 但是, 在光谱信息分类过程中仍然没有考虑土地利用类别由多种地物光谱组成的问题, 其分类精度的提高有限, 对于某些类别还会降低(Smith 等, 2003); 三是采用非统计模式识别的

收稿日期: 2008-01-07; **修订日期:** 2008-10-30

基金项目: 国家自然科学基金(编号: 60673119), 湖南省自然科学基金(编号: 07JJ5066), 湖南省发展改革委员会, 湘财企指[2008]149 号, 湖南省教育厅基金(编号: 06C313)。

第一作者简介: 林剑(1964—), 男, 湖南邵东人, 博士, 副教授, 毕业于中南大学地球探测与信息技术专业, 主要从事遥感图像处理、GIS 等方面的研究, 发表论文 20 余篇。E-mail: lj2110015@163.com。

方法，如决策树分类，通过类别子集形成树的分支决策边界，其实质是通过多子集解决全集的多元统计分布问题(Lucas 等，2007，赵萍等，2005，Conese 等，1993)，该类方法存在子集划分及规则形成困难的问题(Min 等，2005，Pal 等，2003)。

本文从土地利用分类的思想出发，在分析遥感图像土地利用多光谱特征的基础上，提出了一种多光谱遥感图像土地利用分类方法——区域多中心方法，该方法以区域作为分类单元，以训练样本的聚类中心集合表征类别模式，采用基于规则的方法分类，较好地解决了一种类别由多种地物组成，其类别特征不满足一般多元分布的问题。

2 遥感图像多光谱特征分析

2.1 类内空间距离分布

研究特征矢量到类别中心距离的分布是设计分类器算法的基础。如果计算每个像元到类别中心的距离，数值上可能各不相同，为了方便分析，以一定距离区间作为分析单元，先以一定的距离门限值对样本聚类，求取各聚类中心到类别中心的距离，显然二者是一致的。

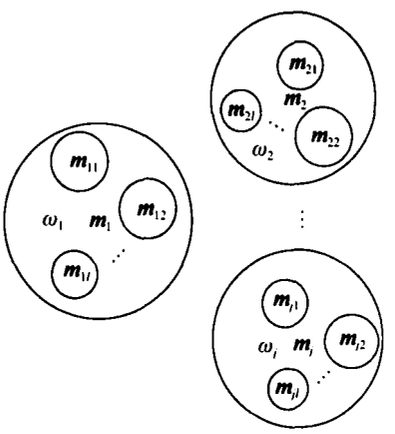

图 1 类别中心与类内中心示意图

设 c 类土地利用类别组成模式集$\{x_1, x_2, \cdots, x_N\}$，$\omega_j$ 类的模式集为 $\{x_i^{(j)}; j=1,2,\cdots,c; i=1,2,\cdots,n_j\}$，其中上角标 j 表示类别，下角标 i 表示类内类样本模式的序号，n_j 为 ω_j 类的模式个数，$\sum_{j=1}^{c} n_j = N$，ω_j 类的类别中心矢量用模式用均值矢量 m_j 表示，即：$m_j = \frac{1}{n_j}\sum_{i=1}^{j} x_i^{(j)}$，$j=1,2,\cdots,c$，对 ω_j 类样本模式以一定的距离门限值聚类，形成 k 个类内中心(图 1)，分别为$\{\omega_{j1}, \omega_{j2}, \cdots, \omega_{jl}\}, l=1,2,\cdots,k$，形成类内中心 ω_{jl} 的模式集为 $\left\{x_i^{(jl)}; j=1,2,\cdots,c; l=1,2,\cdots,k; i=1,2,\cdots,n_l\right\}$，$\omega_{jl}$ 表示 ω_j 类的第 l 个类内中心，n_l 为模式数，$\sum_{l=1}^{k} n_l = n_j$，类内中心的均值矢量分别为 $\{m_{j1}, m_{j2}, \cdots, m_{jl}\}, l=1,2,\cdots,k$，有 $m_{jl} = \frac{1}{n_l}\sum_{i=1}^{n_l} x_i^{(jl)}$，$j=1,2,\cdots,c; l=1,2,\cdots,k$，类内空间距离为 $d_{jl} = \left\| m_{jl} - m_j \right\|$，以 n_l 与 n_j 的百分比为纵坐标，以 d_{jl} 为横坐标作图，称之为类内空间距离分布。

2.2 土地利用类别多光谱特征

实验采用 Landsat TM 长沙市周边 512×512 像元的 4、3、2 波段数据，在城镇用地、林地、耕地和水体 4 种一级土地利用类别中，选取样本进行多光谱类内空间距离分布分析，其样本选取原则为：样本应尽可能涵盖土地利用类别中的各种地物像元。为符合上述原则需要尽可能多地选择样本，样本分布范围要广。根据上述原则每一类别各选样本 8192 个像元，样本选取的大致区域如图 2。

图 3 为土地利用类别类内空间距离分布曲线，聚类采用最大最小值法，其距离门限值为 30，从图 3 可见：(1)各类别中像元光谱值众多，超出其地物种类数目，说明类别中存在大量的混合像元；(2)各类别均存在多个分布较为集中距离段，如水体 30—40 和 60—70 处，反映一种土地利用类别有多种地物组成；(3)水体空间距离分布最为集中，城镇用地相对林地和耕地分布较为集中，但分布的连续性不如林地和耕地。

图 2 样本在遥感图像中的大致区域

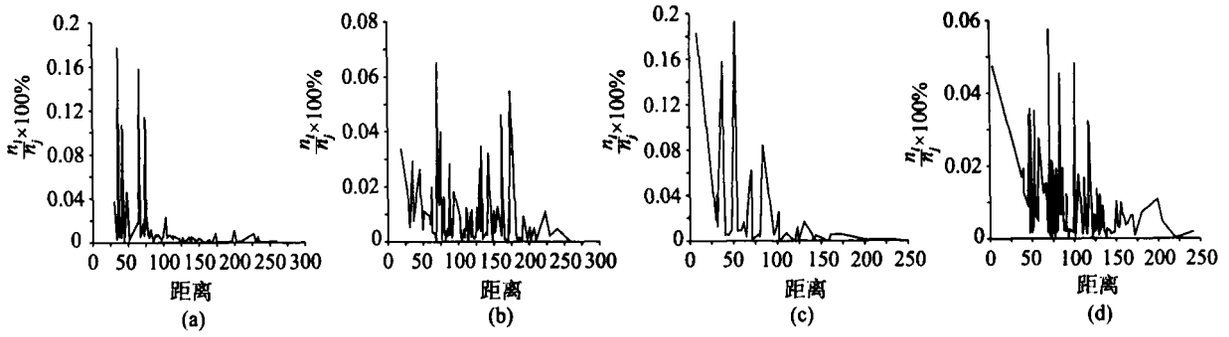

图 3　土地利用类别类内空间距离分布曲线

(a) 水体; (b) 林地; (c) 城镇用地; (d) 耕地

3　区域多中心方法

3.1　方法的基本思路

在土地利用分类体系中，类别的判断标准是根据地物种类及其所占总面积比例划分的，如一级类别城市的标准是：建筑和交通用地占总面积的 2/3 以上，其他任何一种用地不超过总面积的 1/3。依照上述思想，在遥感图像中，以区域为分类单元，单元中像元属于某种类别地物种类的多少及所属某种类别的像元占单元总像元数的百分比进行分类，如图 4 的一个 5×5 区域单元，$\omega_{31},\omega_{33},\omega_{34},\omega_{39}$ 分别表示城镇用地类别中的建筑物、道路、树木和水体，那么，区域单元含有城镇用地类型地物种类为 4 种，属于城镇用地类型像元个数为 18，占单元像元总数的百分比为 72%。

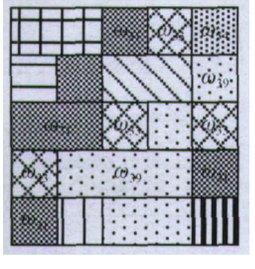

图 4　区域单元类内含类别地物类型示意图

从图 3 可见，用类内中心矢量集合 $\{\boldsymbol{m}_{j1},\boldsymbol{m}_{j2},\cdots,\boldsymbol{m}_{jl}\}$ 表征类别模式更符合土地利用类别的光谱特征分布规律。在此，以类内中心集合表征类别模式，以区域为分类单元，以区域单元含某种类别的类内中心数量及区域单元中所属某种类别的像元占单元总像元数的百分比作为分类准则，称之为区域多中心分类法。

3.2　类别模式的确定

类内中心集合表征土地利用类别模式，中心数是确定类别模式的关键，类别模式选择的原则是：使类内距最小、类间距最大。通过计算不同中心数形成的类别模式的类内、类间距确定中心数。

如图 1，采用单一中心表征类别模式时，类内距定义为：$d_\omega=\sum_{j=1}^{c}\sum_{i=1}^{n_j}\left\|\boldsymbol{x}_i^{(j)}-\boldsymbol{m}_j\right\|^2$，式中，$\boldsymbol{m}_j$ 表示 ω_j 类的模式均值矢量。

类间距定义为：$d_B=\frac{1}{c}\sum_{j=1}^{c}(\boldsymbol{m}_j-\boldsymbol{m})'(\boldsymbol{m}_j-\boldsymbol{m})$，式中，$\boldsymbol{m}$ 为总的模式平均矢量，$\boldsymbol{m}=\frac{1}{N}\sum_{i=1}^{N}\boldsymbol{x}_i$。

采用类内中心集合表征类别模式时，定义各模式到所属类内中心距离平方和为多中心类内距离：

$$d_{\omega\omega}=\sum_{j=1}^{c}\sum_{i=1}^{n_j}\left\|\boldsymbol{x}_i^{(jl)}-\boldsymbol{m}_{jl}\right\|^2。$$

多中心类间距离定义为：

$$d_{B\omega}=\frac{1}{c\times k}\sum_{j=1}^{c}\sum_{l=1}^{k}(\boldsymbol{m}_{jl}-\boldsymbol{m})'(\boldsymbol{m}_{jl}-\boldsymbol{m})。$$

采用 1.2 节实验样本，对各类别用不同中心数进行C均值聚类形成不同的多中心，其多中心类内、类间距离如表 1。

以类内距最小、类间距最大为原则选取中心数，根据表 1，中心数可在 10—120 的范围内选取。

3.3　土地利用类别区域多中心特征

区域多中心特征指区域单元含某种类别的类内中心数特征及区域单元中属于某种类别的像元占单

表 1　不同类内中心数的类内、类间距离

中心数	1	2	5	10	25	30	50	100	120	200
类内距	76.91	78.97	61.85	40.16	28.71	25.45	18.97	13.67	12.99	9.60
类间距	103.42	31.38	71.18	109.59	108.53	102.61	128.14	112.49	147.51	97.34

元总像元数的百分比特征。实验方法如下:

(1) 选取各类别训练样本, 用 C-均值法形成多中心, 删除像元数小于一定门限值的中心, 排除图像噪声和占总面积比例极少的地物影响, 以调整后的中心集合作为类别分类模式, 并求取像元到中心的最小距离 $d_{\min}$;

(2) 在各类别中任选一定大小的样本区域, 区域中每一个像元对各类内中心以 $d_{\min}$ 距离为门限值归类, 即 $\|x-m_{jl}\| \leqslant d_{\min}$, $x \in \omega_j$, 区域单元含 ω_j 类的 ω_{jl} 类内中心。

(3) 统计区域单元所含各类别的类内中心数及像元类别百分比。

3.3.1 不同训练样本的区域多中心特征

根据 2.2 节中样本选取原则, 选取 A、B、C 3 组训练样本, 各组样本数量分别为 8192、4096 和 1024 个像元, C - 均值的初始类为 50, 删除像元数小于训练样本总数 0.1%的中心, 然后, 在各类别区域中任取 11 × 11 的区域单元样本。区域单元多中心特征如表 2 和表 3。

表 2 训练样本为 A 组的区域单元多中心特征

	水体样本	林地样本	城镇样本	耕地样本
水体类	10, 100%	0, 0	2, 21.9%	0, 0
林地类	0, 0	6, 100%	3, 23.5%	1, 7.4%
城镇类	0, 0	1, 3.3%	19, 100%	0, 0
耕地类	0, 0	0, 0	3, 4.1%	11, 100%

注: 首项表示类别类内中心数, 后项表示所占比例

表 3 训练样本为 C 组的区域多中心特征

	水体样本	林地样本	城镇样本	耕地样本
水体类	14, 100%	0, 0	4, 19.8%	0, 0
林地类	0, 0	8, 100%	2, 29.7%	1, 0.8%
城镇类	0, 0	0, 0	25, 100%	0, 0
耕地类	1, 0.8%	0, 0	2, 3.2%	11, 95.0%

从表 2 和表 3 可见, 对于不同的训练样本清楚地表明: 区域单元源自某种类别, 单元含有该类别的类内中心数、像元属于该类别的百分比远远大于其他类别。

3.3.2 区域单元大小不同的区域多中心特征

采用 B 组样本, 区域单元的大小分别为 16 × 16、7 × 7。区域单元多中心特征如表 4。

从表3—表5可见, 对于不同的区域单元大小清楚地表明: 区域单元源自某种类别, 单元含有该类别的类内中心数、像元属于该类别的百分比远远大于其他类别。

表 4 区域单元大小为 16×16 的区域多中心特征

	水体样本	林地样本	城镇样本	耕地样本
水体类	23, 99.6%	0, 0	0, 0	2, 15.6%
林地类	0, 0	10, 97.6%	0, 0	0,0
城镇类	4, 51.1%	2, 41.5%	27, 98.4%	3, 4.7%
耕地类	0, 0	4, 3.9%	0, 0	25, 98.8%

表 5 区域单元大小为 7×7 的区域多中心特征

	水体样本	林地样本	城镇样本	耕地样本
水体类	10, 100%	0, 0	0, 0	2, 6.1%
林地类	0, 0	4, 93.0%	0, 0	0,0
城镇类	2, 38.7%	2, 40.0%	19, 100%	0, 0
耕地类	0, 0	0, 0	0, 0	12, 100%

3.4 方法流程

多光谱遥感图像土地利用分类区域多中心方法流程如图 5。

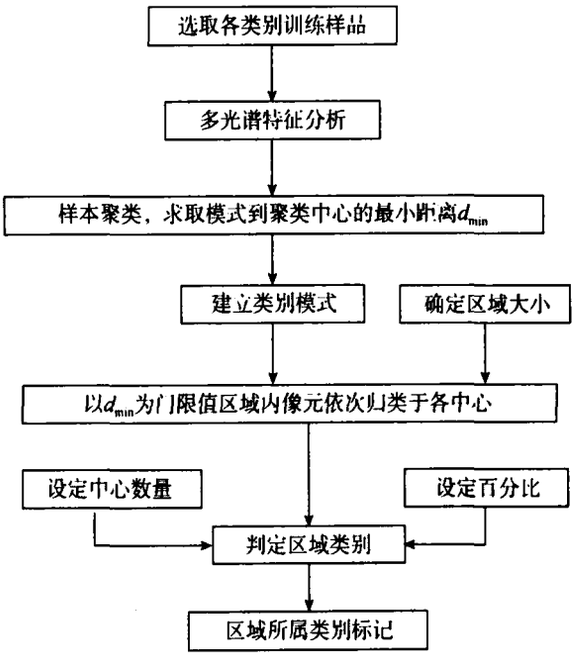

图 5 区域多中心法流程图

4 实 验

实验数据如图 2, 选取城镇用地、林地、耕地、水体和裸地 5 种一级土地利用类别进行实验研究, 在分类后的图像中, 分别用绿色、红色、黄色、蓝色和白色表示, 不可分区域用黑色表示。

各种方法采用一致的训练样本选择和精度评价方法。训练样本选取原则为: 样本应尽可能涵盖土地利用类别中的各种地物像元, 用目视的方式尽可能多的选取已知区域像元; 精度评价方法为: 分类

后图像中随机选取 100 个点，根据目视解译的结果像统计分类误差。

4.1 常用方法的分类

图 6 为常用的土地利用分类方法的分类结果，其中图 6(a)为最大似然法(Benediktsson 等，1997)，图6(b)为FasART神经网络法(林剑等, 2002)，图6(c)决策树分类法(赵萍等，2005)，图 6(d)纹理特征和光谱特征基于分类器融合分类法(林剑等，2004)，其分类结果如表 6。

从表6可见，基于多中心的神经网络分类方法和基于决策树的分类方法对土地利用类别像元光谱特征较为分散的林地和耕地较最大似然法的分类精度有所提高，光谱特征与基于区域的纹理特征融合分类的总体分类精度有所提高，但提高的幅度不大。

4.2 区域多中心方法不同判断准则的分类

区域大小取 5×5，通过训练样本(A 组)形成城镇用地、水体、耕地、林地和裸地的模式中心数分别为 50, 20, 50, 50 和 10，用不同的中心数门限值和百分比门限值进行实验，其实验结果如图 7，分类精度如表 7。

从图7(d)可见，当中心数门限值为2时，不可分区域明显增多，但分类精度变化不大，主要因为一是区域较小，区域内像元相对集中，二是聚类中心数较大，判断像元是否属于类别的最小距离较小。从表 7 中可见分类规则的变化引起的精度变化不超过 1%，说明区域多中心法较容易选择分类规则门限值。图 7 对比图 6，类别中的斑点明显减少；表 7 对比表 6 分类精度提高 4%左右。

4.3 不同训练样本及类别模式的分类

图 8 为不同训练样本及同一组训练样本模式中心数不同的分类结果图，其区域大小为 5×5，中心门限值为 1，百分比门限值为 55%，表 8 为分类精度表。图 8(a)和图 7(c)为 B 组样本模式中心数不同的分类结果，从图中难以看出其分类的差别，在表 8

表 6　常用方法分类精度

/%

分类方法	水体	林地	城镇	耕地	裸地	平均
最大似然	85.6	84.1	76.3	82.9	86.5	83.08
神经网络	87.7	86.8	72.4	85.6	85.3	83.56
决策树法	90.2	85.7	74.6	84.2	85.1	83.96
融合分类	87.0	85.2	81.7	84.1	85.9	84.78

表 7　不同中心数和像元类别百分比门限值的分类精度

/%

图 7	水体	林地	城镇	耕地	裸地	平均
(a)	87.5	88.3	86.8	88.7	85.9	87.44
(b)	87.1	88.9	87.7	89.1	85.7	87.70
(c)	87.5	87.8	86.8	88.8	86.0	87.38
(d)	87.3	87.5	86.6	88.0	85.2	86.92

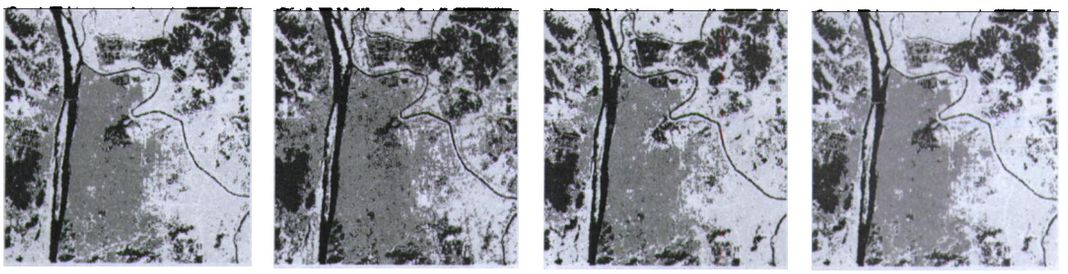

(a)　(b)　(c)　(d)

图 6　常用土地利用分类方法结果图

(a) 最大似然法; (b) 神经网络法; (c) 决策树法; (d) 纹理与光谱信息多分类器融合分类法

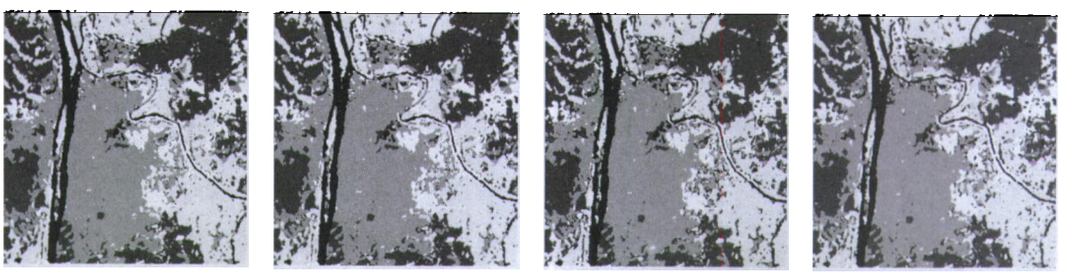

(a)　(b)　(c)　(d)

图 7　不同中心数与百分比门限值的区域多中心方法分类结果图

(a) 中心数 1，百分比 50%; (b) 中心数 1，百分比 55%; (c) 中心数 1，百分比 60%; (d) 中心数 1，百分比 45%

表 8 不同训练样本及类别模式的分类精度

/%

图 8	水体	林地	城镇	耕地	裸地	平均
(a)	88.5	87.8	86.8	89.3	86.2	87.72
(b)	88.2	87.6	87.0	88.9	85.3	87.40
(c)	87.9	88.3	86.4	89.2	86.0	87.56
(d)	86.4	88.5	88.7	89.0	84.1	87.34

中其精度误差相差不超过 0.5%，充分说明了模式中心数在一定的范围变化对分类精度影响很小；图 7 和图 8 中有 3 组不同的训练样本，从表 7 和表 8 中可见其平均精度相差不超过 1%，说明区域多中心方法对训练样本的选择要求不高。

4.4 区域多中心方法单一类别的提取

图 9 为遥感图像中单一土地利用类别提取的结果，在分类的过程中只选取单一类别的训练样本，从结果图中可见类别中几乎不存在斑点，与目视遥感图像土地一级分类结果十分接近。其区域多中心方法参数及提取精度如表 9，从表中可见各类别的精度与表 7 和表 8 相比均有提高，平均精度高 3%左右。这是由于根据类别的尺度特征可以选择不同的分类区域的大小，当区域分类区域增大时有利于中心数门限值的控制，从而提高分类的精度。

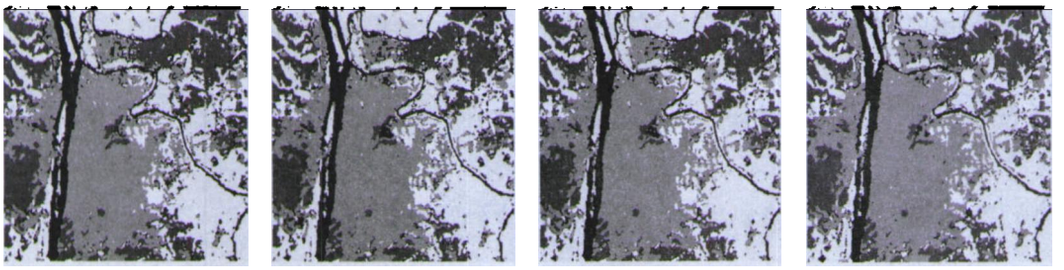

(a) (b) (c) (d)

图 8 不同训练样本及类别模式的区域多中心方法分类结果图

(a) B 组，模式 50,20,50,50,10; (b) B 组，模式 50,30,70,70,20; (c) B 组，模式 60,30,60,60,20; (d) C 组，模式 50,20,50,50,10

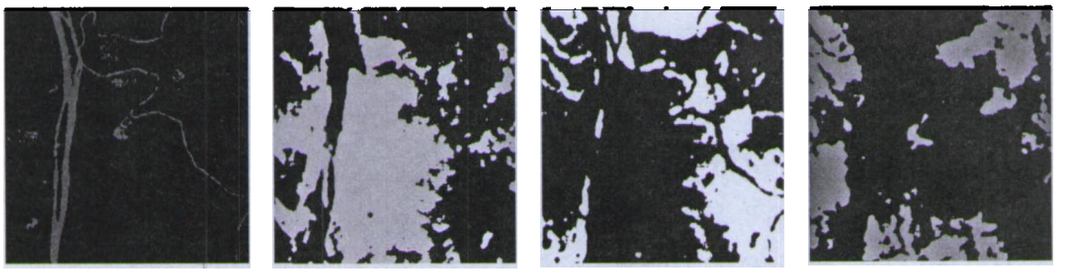

(a) (b) (c) (d)

图 9 区域多中心法单一类别识别结果图

(a) 水体; (b) 城镇用地; (c) 耕地; (d) 林地

表 9 单一类别提取区域多中心方法参数及精度表

	区域大小	模式中心数	中心数门限值	百分比门限值	精度/%
水体	3×3	20	1	55	89.6
城镇	11×11	50	3	60	90.1
林地	9×9	50	4	60	89.7
耕地	9×9	50	3	60	91.2

5 结 论

本文提出了一种新的多光谱遥感图像土地利用分类方法——区域多中心法，以类内中心集合表征类别模式，较好地解决了土地利用类别由多种地物组成、类别模式不满足多元正态分布的问题，提高了多光谱特征较为分散的类别分类精度；以区域单元像元含有类别中心的数量及属于某一类别的像元占单元像元总数的百分比作为分类准则，体现了土地利用分类体系以地物种类及其所占总面积比例划分的基本思想，有机地融合了多光谱遥感图像的区域信息与光谱信息；由于类别区域单元多中心特性差异大，分类规则的建立及训练样本的选择易于实现，较好地解决了决策树分类方法训练子集的划分及决策边界确定的问题；该方法同时可用于单一类别提取，可以针对不同类别的特点采用不同的分类

规则。区域多中心法可以提高多光谱遥感图像土地利用分类精度4%—6%。

REFERENCES

Alberti M, Weeks R and Coe S. 2004. Urban land cover change analysis in Central Puget Sound. *Photogrammetric Engineering and Remote Sensing*, **70**(9): 1043—1052

Benediktsson J A, Sveinsson J R and Swain P H. 1997. Hybrid consensus theoretic classification. *IEEE Trans. Geosci. Remote Sens*, **35**(4): 833—843

Bruzzone L, Cossu R and Vernazza G. 2004. Detection of land-cover transitions by combining multidate classifiers. *Pattern Recognition Letters*, **25**(13): 1491—1500

Chen Q X, Luo J C, Zhou C H, Zheng J, Lu X J and Shen Z F. 2004. Classification of remotely sensed imagery using multi-features based approach. *Journal of Remote Sensing*, **8**(3): 239—245

Cingolania A M, Renisona D, Zak M R and Cabido M R. 2004. Mapping vegetation in a heterogeneous mountain rangeland using landsat data: an alternative method to define and classify land-cover units. *Remote Sensing of Environment*, **92**(1): 84—97

Conese C, Gilabert M A, Maselli F and Bottai L. 1993. Topographic normalization of TM scenes through the use of an atmospheric correction method and digital terrain models. *Photogrammetric Engineering and Remote Sensing*, **59**(12): 1745—1753

Gislason P O, Benediktsson J A and Sveinsson J R. 2006. Random Forests for land cover classification. *Pattern Recognition Letters*, **27**(2): 294—300

Kuemmerle T, Radeloff V C, Perzanowski K and Hostert R. 2006. Cross-border comparison of land cover and landscape pattern in Eastern Europe using a hybrid classification technique. *Remote Sensing of Environment*, **103**(1): 449—464

Lin J, Bao G S, Jing R Z and Huang J X. 2002. A study of fasART neuro-fuzzy networks for supervised classification of remotely sensed images. *Journal of Image and Graphics*, **7**(12): 186—190

Lin J, Bao G S, Wang R S and Wang X. 2004. Fusion spectrum and texture information of RS image based on decomposing fuzzy density. *Acta Electronica Sinica*, **32**(12): 2028—2030

Lucas R, Rowlands A, Brown A, Keyworth S and Bunting P. 2007. Rule-based classification of multi-temporal satellite imagery for habitat and agricultural land cover mapping. *ISPRS Journal of Photogrammetry & Remote Sensing*, **62**(3): 165—185

Luo J C, Wang Q M, Ma J H, Zhou C H and Liang Y. 2002. The EM-based maximum likelihood classifier for remotely sensed data. *Acta Geodaetica Et Cartographic Sinica*, **31**(3): 234—239

Min X, Pakorn W V and Manoj K A. 2005. Decision tree regression for soft classification of remote sensing data. *Remote Sensing of Environment*, **97**(3): 322—336

Pal M and Mather P M. 2003. An assessment of the effectiveness of decision tree methods for land cover classification. *Remote Sensing of Environment*, **86**(3): 554—565

Smith J H, Stehman S V, Wickham J D and Yang L M. 2003. Effects of landscape characteristics on land-cover class accuracy. *Remote Sensing of Environment*, **84**(2): 342—349

Yuan F, Sawaya K E, Brian C and Bauer M E. 2005. Land cover classification and change analysis of the Twin Cities (Minnesota) Metropolitan Area by multitemporal Landsat remote sensing. *Remote Sensing of Environment*, **98**(2): 317—328

Zak M R and Cabido M. 2002 Spatial patterns of the Chaco vegetation of central Argentina: Integration of remote sensing and phytosociology. *Applied Vegetation Science*, **5**(2): 213—226

Zhao P, Fu Y F, Zheng L G and Feng X Z. 2005. Cart-based land use/cover classification of remote sensing image. *Journal of Remote Sensing*, **9**(6): 708—716

Zhu H J. 2006. Research on classification and representation of residential change for the automatic retrieval incremental information. *Journal of Hunan University of Science & Technology*, **21**(3): 65—68

附中文参考文献

陈秋晓, 骆剑承, 周成虎, 郑江, 鲁学军, 沈占锋. 2004. 基于多特征的遥感影像分类方法. 遥感学报, **8**(3): 239—245

林剑, 鲍光淑, 敬荣中, 黄继先. 2002. FasART 模糊神经网络用于遥感图像监督分类的研究. 中国图象图形学报, **7**(12): 186—190

林剑, 鲍光淑, 王润生, 王欣. 2004. 基于模糊密度分解的遥感光谱和纹理信息的融合. 电子学报, **32**(12): 2028—2030

骆剑承, 王钦敏, 马江洪, 周成虎, 梁怡. 2002. 遥感图像最大似然分类方法的 EM 改进算法. 测绘学报, **31**(3): 234—239

赵萍, 傅云飞, 郑刘根, 冯学智. 2005. 基于分类回归树分析的遥感影像土地利用/覆被分类研究. 遥感学报, **9**(6): 708—716

朱华吉. 2006. 面向增量信息自动化提取的居民地时空变化分类研究. 湖南科技大学学报, **21**(3): 65—68